DTU Library

Thermal behavior of a combi-storage in a solar-ground source heat pump system for a single-family house

Zhang, Changxing; Nielsen, Elsabet; Fan, Jianhua; Furbo, Simon

Thermal behavior of a combi-storage in a solar-ground source heat pump system for a single-family house

Changxing Zhang[a,b,*], Elsabet Nielsen[b], Jianhua Fan[b,*], Simon Furbo[b]

[a]*Shandong Key Laboratory of Civil Engineering Disaster Prevention and Mitigation, Shandong University of Science and Technology, Qingdao 266590, PR China*

[b]*Department of Civil Engineering, Technical University of Denmark, Brovej 118, 2800 Kgs.Lyngby, Denmark*

Abstract: Experimental investigations on thermal behavior of a combined solar and ground source heat pump (SGHP) system for a single-family house are presented. The SGHP system was installed at the Lyngby campus of Technical University of Denmark. Detailed experiments were carried out on the system in 2019 under real weather conditions covering domestic hot water (DHW) consumption and space heating (SH) demand. Depending on the contributions of the energy inputs to the combi-storage, five typical daily operation modes are classified. The focus of the investigations is on the dynamic thermal behaviors of the heat storage under different operating conditions. When the combi-storage was primarily heated by solar energy, the inlet stratifier in the storage performed well, ensuring thermal stratification and a good utilization of solar energy. Water temperature in the storage reached up to about 68℃ at the end of the solar heating process. When the combi-storage was primarily heated by the ground heat, the water temperature near the outlet for SH was kept at a temperature range from 26℃ to 31℃ in the heating process to ensure the outlet temperature level of SH, and the water temperature near the outlet for DHW was in the temperature range 47℃~51℃ in DHW volume. When there was no heat input to the combi-storage, the pre-stored heat can meet the daily heating demand, and the number of days on this mode was up to 9.4% of the total experimental days. The paper gives valuable inputs for researchers and engineers who plan to integrate the combi-storage in a renewable heating system with solar collectors and ground source heat pumps.

4   ──────────────────────
5   *Corresponding authors.
6   *E-mail addresses:* jif@byg.dtu.dk (J. Fan), zcx952@163.com (C. Zhang)

1. Introduction

8   With an increased popularity and availability of renewable energy sources, there are more and

9   more households heated by heat pump and solar energy systems. Compared with air source heat

10   pump system, a ground source heat pump (GSHP) system can achieve a higher coefficient of

11   performance (COP) because the ground provides more favourable temperatures, and experiences

12   less temperature fluctuations than the ambient air. Therefore, GSHP system is widely applied for

13   heating/cooling of buildings, snow melting and in other fields[1][2][3][4]. Moreover, horizontal

14   ground heat exchanger (HGHE) in GSHP systems is used for heating a single family house due to

15   its economic advantage[5][6], and its performance was also validated by experiments [7][8] and

16   numerical models [9]. Accurate artificial algorithms provide a fast tool for predicting and evaluating

17   GSHP system with HGHE[10][11][12][13][14][15]. Different with the single source solar energy

18   utilization system[16][17], the heating systems combining solar energy and GSHP system show

19   better thermal performance[18]. In the investigations on the energetic performances of combining

20   systems for a single family house (SFH45) in Strasbourg, the highest seasonal performance factor

21   (SPF) of 6.5 was achieved by a combination of solar and ground source heat pump (SGHP) system,

22   which was 54.8% higher than that of the combined solar and air source heat pump system[19]. The

23   survey in Ref. [20] shows that the SGHP system accounts for about 10.5% of the heat source for

24   residential building.

25   Generally, SGHP system is equipped with a thermal energy storage due to the time differences

26   between heat production and household heat demand. The storage devices are usually based on

27   sensible heat, using water as a short-term heat storage and the ground as a seasonal heat storage[21].

28   As the most frequently used heat storage medium, water is excellent due to its large specific heat,

1   low price, nontoxicity, and chemical inertia. The sensible heat storage capacity of water is

2   approx.70 kWh/m^3 for household heating in the temperature range of $20°C$-$80°C$. Therefore, short-

3   term heat storages using water are economically attractive for residential heating inclusive domestic

4   hot water (DHW) and space heating (SH). Based on the monitoring investigation on a SGHP

5   system in a new housing complex in Satigny, Switzerland, 37% of the energy supplied to the flats

6   went through the storage before use [22]. As the core component in SGHP system, the water storage

7   tank can not only shave the demand peak, also store the solar heat produced in the period without

8   heat demand, which will effectively shorten the operation times of the ground source heat pump

9   system. Undoubtedly, the storage tank plays an important role in the heating system by overcoming

10 the mismatch of heat production and consumption and improving the system performance[23][24].

11 In the SGHP system for a school building, the underground tank for short-term storage of heat was

12 proven effective to improve the system performance by charging/discharging cycle in three months

13 of the year[25]. Dai et al. [26] studied the influence of operation modes on the heating performance

14 of a SGHP system, and validated that the solar fraction of SGHP system kept steady in all the

15 modes because of the ability to store a portion of the solar heat in the water tank.

16   More efforts have been done to investigate thermal behavior of the storage tank in SGHP system.

17 Thermal stratification in the storage tank is one of the key factors determining thermal performance

18 of the heating system[27]. Thermal stratification could be destroyed by mixing in the tank due to

19 incoming jet flows. Based on the measurements on eight marketed solar domestic hot water

20 (SDHW) systems, Furbo S [28] concluded that the thermal performance of SDHW system was

21 primarily determined by the design of the hot water tank. Furthermore, the combi-storage was found

22 to be the most suitable in the solar heating systems. In order to investigate the influence of different

23 DHW heating loads and consumption patterns, Knudsen S [29] tested a low-flow SDHW system

24 with a mantle tank and a high-flow SDHW system with an internal heat exchanger spiral in the heat

25 storage. The results showed that a mixing rate of 40% caused a reduction of around 10% in the net

26 utilized solar energy for the mantle tank systems while the reduction for the spiral tank systems was

about 16%. The mixing during draw-offs should be avoided in order to limit its negative impact on the system performance.

Many works focused on development of new stratification devices. Theoretical and experimental investigations on multilayer fabric stratification pipes and inlet stratifiers for solar tanks were carried out by Computational Fluid Dynamics (CFD) simulations and Particle Image Velocimetry (PIV) measurements[30], and enhancement of thermal stratification via obstacles in vertical mantled hot water tank was studied experimentally[31]. Dragsted J et al. [32] experimentally proved that two types of inlet stratifiers had an ability to create stratification in the tank under different test conditions, and that thermal stratification could be built up in a storage tank during charge. Padovan R et al.[33] developed the ESP-r model of the combi-storage, and the model was validated against experimental data. Based on CFD simulation, Moncho-esteve IJ et al. [34] found that modifications of the simulated inlet devices affected the stratification level, and a sintered bronze conical diffuser could improve stratification compared to a conventional bronze elbow inlet. The use of low inflow, smoothed inlet velocity and upwards inflow at the top of the tank enhanced stratification.

Different from the aforementioned DHW systems or space heating (SH) systems, solar combisystem is designed to meet the residential heating demand for DHW and SH, which is popular for single-family houses. Furthermore, solar cobmisystems are becoming more and more advanced because of the improvement on thermal stratification in the storage tanks and controlling strategies. By comparing thermal performance of four highly advanced and differently designed solar combisystems, Drück and Hahne [35] concluded that the system performance was subject to low heat losses and a small auxiliary volume in the combi-storage with a low set point temperature. Investigations were carried out to improve thermal stratification of the storage tank, for example, by the low flow principle and inlet stratification devices. Pauschinger et al. [36] presented that low flow and inlet stratifiers can improve system performance of a solar combisystem by 3%. Jordan [37] proposed that the thermal performance of solar combisystem was increased by about 1-2% by

using a stratification manifold instead of a fixed inlet in the combi-storage. The investigated system

had a solar fraction of about 25%. Lorenz [38] showed that thermal performance of a solar

combisystem was improved by 25%-35% by replacing the non- stratified tank with a highly

stratified combi-storage. Andersen E et al. [39] made an investigation on thermal performance of

Danish solar combisystems in single-family houses, and the measurements showed that thermal

performance was highly influenced by the demand during the summer (from the middle of May to

the middle of September). Parametric studies on two combisystems showed that the thermal

performances could be significantly improved by design changes of the combi-storage, such as

maintaining high thermal stratification, keeping the return temperature from the SH loop low, and

making the tank well insulated, etc. Durisch W et al. [40] investigated the feasibility of improving

thermal performance of both SDHW systems and solar combisystems by using two draw-off levels

from the combi-storages. The results showed that about 5% increase of thermal performance can be

obtained with a second draw-off level for the combi-storage. Andersen E and Furbo S [41] carried

out theoretical investigations on three differently designed solar combisystems with Danish weather

data. With the net utilized solar energy as a function of DHW, SH and the relative return inlet

height from the SH loop, the best performing system with improvement of 7-14% was achieved by

the tank-in-tank combi-storage with inlet stratifiers in both the solar collector loop and the SH loop.

Besides the aforementioned investigations on the storage tanks, the influences of the system size

and the control system of the solar collector loop were also studied[42]. By monitoring three

temperatures of two separated tanks, Bois J et al. [43] analyzed detailed behavior and efficiency of a

solar combisystem in the whole year based on an existing control algorithm. It was seen that higher

energy savings of 34%-70 % could be obtained by reducing energy demands or increasing solar

collector area. El-baz W and Tzscheutschler P [44] experimentally investigated a ground source

heat pump system with a combi-storage for household SH and DHW consumption. The result

showed that DHW/SH sensor position influenced the number of starts and might lead to short

cycling, and that tank set temperature had a direct impact on COP of the heat pump. Based on

simulations of solar and air source heat pump systems with the combi-storage, Haller MY et al. [45]

recommended that the position of the DHW sensor for charging control must be placed at a safe

distance from the SH zone of the storage, which depended on the stratification efficiency of the

storage and on the mass flows used for storage charging and discharging.

In most of the investigations, the heat storage tanks were tested in limited time periods under a

controlled lab environment, thus long term thermal behavior of the storages under realistic

boundary conditions are rarely studied. This paper aims to investigate a SGHP system for a single

family house with a tank-in-tank combi-storage for DHW and SH under real environment. The

tank-in-tank combi-storage has a better surface to volume ratio compared to traditional combi-

storage tanks. Since there is only one device where the ground and solar heat have to connect,

hydraulics and control of the system could be simplified[46]. The combi-storage was equipped with

an inlet stratifier for the solar collector loop and four inlet/outlet pipes at variable heights for the

ground heat pump. Advanced control strategy was implemented in the system. The aim of the

design and the control strategy is to secure a high degree of thermal stratification in the storage and

a high efficiency of the heating system. This paper presents for the first time long-term

experimental investigations of the combi-storage under real boundary conditions.

This paper has focus on the dynamic thermal behavior of the combi-storage under different

operating conditions. The charging/discharging characteristic of the combi-storage will be

investigated in details based on dynamic interaction between supply and demand. As shown in

Fig.1, the interplay between the combi-storage and the heating sources inclusive solar heat and the

ground heat pump will be analysed with variable heating demands for DHW and SH in the climate

condition throughout the year. The five operation modes of the combi-storage under the control

strategy will be investigated in details. Furthermore, thermal stratification in the combi-storage and

the influence of the two heat sources will be elucidated by means of temperature measurements in

the tank. The investigations will also demonstrate the functions of the combi-storage, inclusive heat

demand peak shaving, storage of surplus solar heat and operation stability of the system.

1

2

3
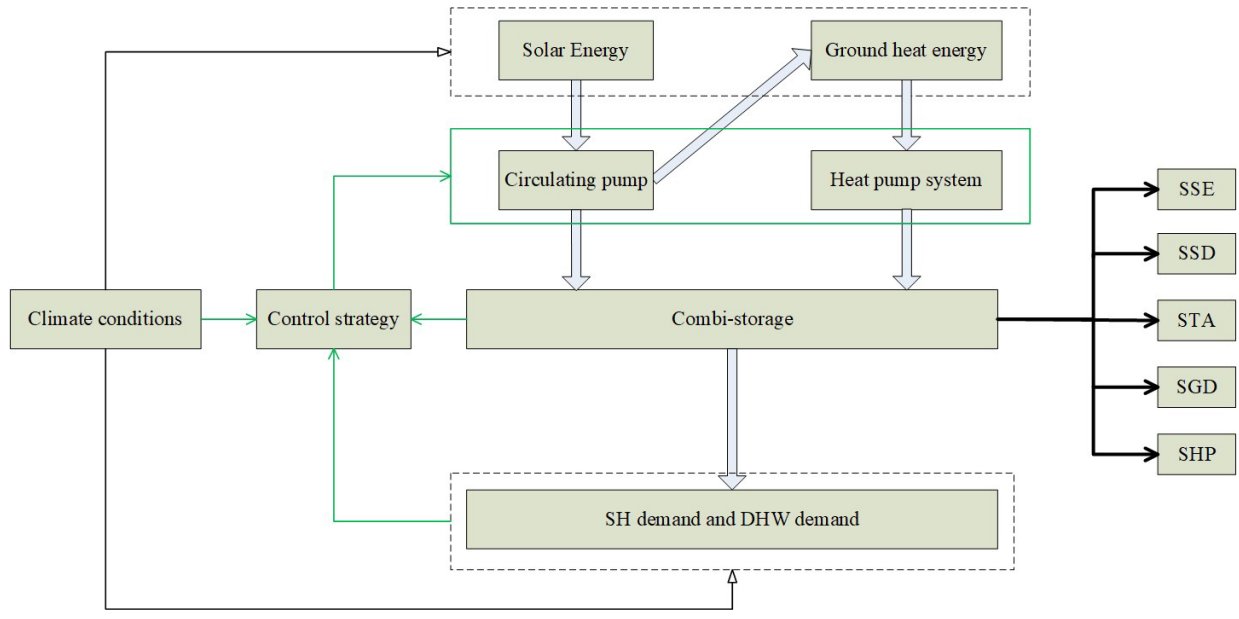
4   **Fig.1** The energy supply/demand interactive relations and dynamic thermal response of the
5   combi-storage

2. The experiment

2.1 The SGHP system

8   The SGHP system was installed and measured at the Lyngby campus of Technical University of

9   Denmark. The SGHP system is composed of a tank-in-tank combi-storage, a water-to-water heat

10 pump, vacuum tube solar collectors and HGHE. Automated draw offs of DHW and SH in the

11 system is used to replicate a realistic demand of a single-family house under real climatic conditions.

12 Fig.2 illustrates an overview of the SGHP system with locations of measurement and controller

13 sensors, and the descriptions of the main components are listed in Table.1. For the solar collector

14 loop shown in Fig.1, the solar collectors provide heat for the combi-storage and HGHE by parallel

15 coupling two plate heat exchangers, direct solar usage is prioritized to heat the combi-storage than

16 the heat pump. The HGHE, which is located at a level of 1 m below the lawn surface outside the

17 test house, acts as the heat sink in the regeneration loop, and as the heat source of the auxiliary

18 heating loop. Two circulating pumps (P5 and P6) and the single stage variable- frequency piston

19 compressor were integrated in the heat pump cabinet.

Solar collector

Tank-in-tank

TA1
T1
T3
TA4
T4
T6
TA2

T25
T28
T29
T26
T30
T31
T27
T32

T4

T12

F3
M8

Space heating

F1

P1
M7
P2
T3
T2

F2
M2

TH
TC

T11

Domestic hot water

T19
F7

T1X
T4X
T3X
T2X

M5
M4
T19X

P5
T17X
M6

T18
F5

T2
T1

Auxiliary heating

Heat pump, 3-12 kw

T9

T7
T8
P6

T18X
T20X

T14
T13

F6
TA3

P3

Ground source heat exchanger

Motor valve/magnetic valve
Three way motor valve
Thermostatic valve
Pump
Flow meter
Temperature sensor for hp control system
Temperature sensor for sc control system
Temperature sensor for monitoring

a) The SGHP system

b) Combi-storage and heat pump

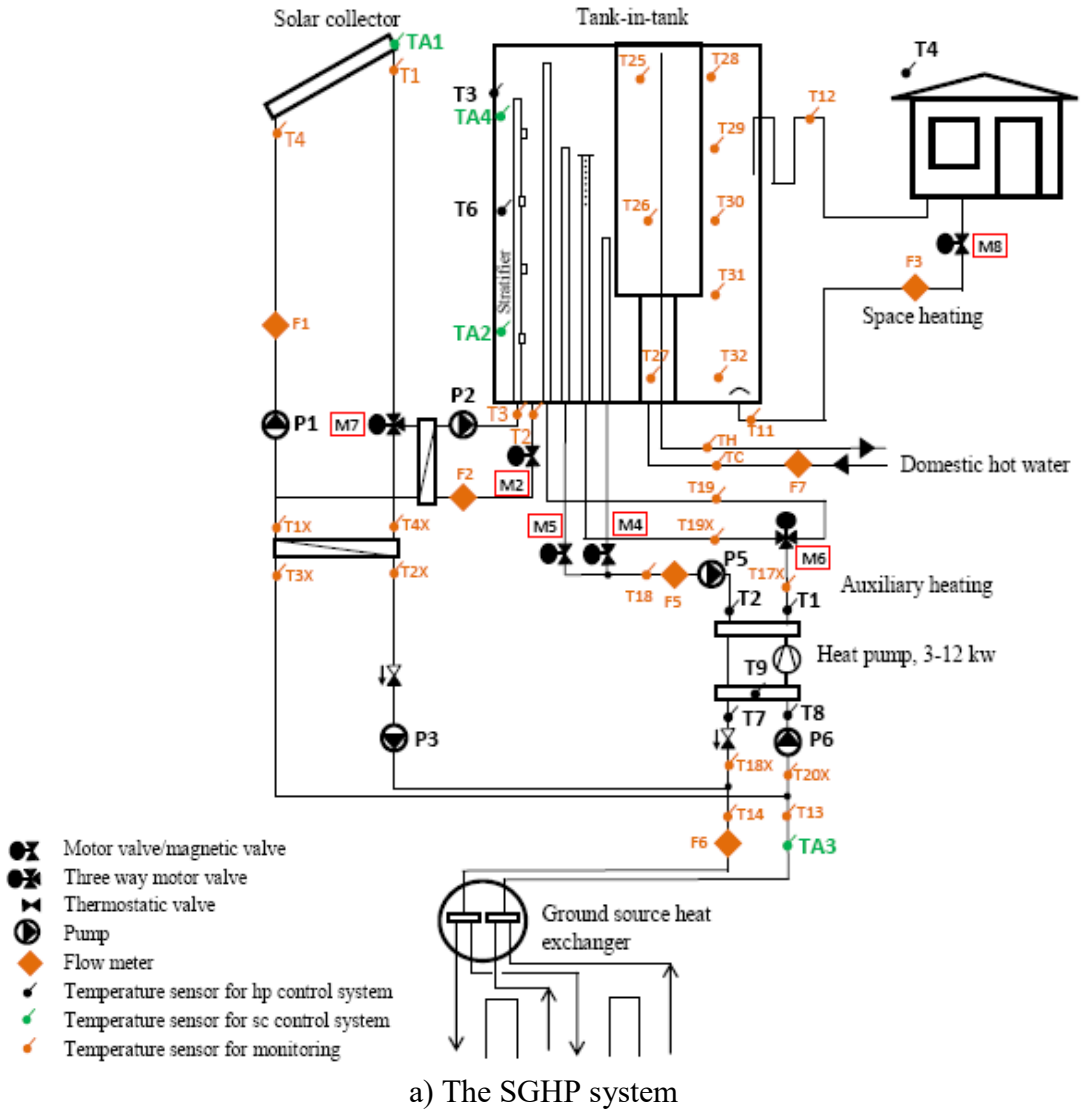**Fig.2** An overview of the SGHP system with measurement and controller sensors locations

1
2
3
4
5   **Table 1** The main components of the SGHP system

Component	Description
Solar collector	9.6 m^2, Evacuated tubular collectors, type Thermomax HP 450, Kingspan, the parameters to calculate collector efficiency [47]
The combi-storage (Tank-in-tank)	Total volume 0.725 m^3, inner domestic water tank 0.175 m^3, 5 ports
Plate heat exchangers	Heat transfer area 0.5 m^2, 9 kW capacity
Heat pump	HGX 12P/110-4s, heating capacity 3-12 kW, R134a
Circulation pump	P1: NMT PLUS 25/80-180, IMPPUMPS
	P2: UPS 25-40-180,Grundfos
	P3: UPS 25-60-180, Grundfos
	P5:Alfa 125-60-180,Grundfos
	P6:Magna 25-60-180,Grundfos
Horizontal ground heat exchanger	Total length 240 m; Cover area 8.5 m x 30 m; HDPE pipe outside diameter/wall thickness 40 mm/2.5 mm
Controller	LMC 320 for the auxiliary loop; UVR63 for the solar collector loop

6

7   A big uninsulated buffer tank and a cooling system combined with an insulated storage tank

8 acted as heat sink for both the SH loop and the DHW loop[48]. The typical daily accumulated heat

9 demand for SH and DHW in winter is shown in Fig.3. The DHW consumption of approximate 5

10 kWh was tapped every day by setting three-time DHW draw offs of about 7.5 l/min. For yearly SH

11 demand for around 2800 kWh, heat was drawn from the combi-storage by activing the circulating

12 flow rate of about 5 l/min every day, and the setting time slots for discharging varied from month to

13 month in the heating season. In order to evaluate thermal performance of the SGHP system, the

14 absolute temperatures at different key locations, the volume flow rates of the seven loops and

15 electricity consumption of different component were recorded with an interval of 1 minute. As the

16 temperature sensors shown in Fig.1, the green mark points (TA1—TA4) were used in the

17 controlling system for solar heating supply, the black mark points (T1—T9) were used to control

18 heat pump system and protect the safety operation of the piston compressor, and the others (Orange

19 mark points) were all used to monitor the key temperatures in the combi-storage and evaluate the

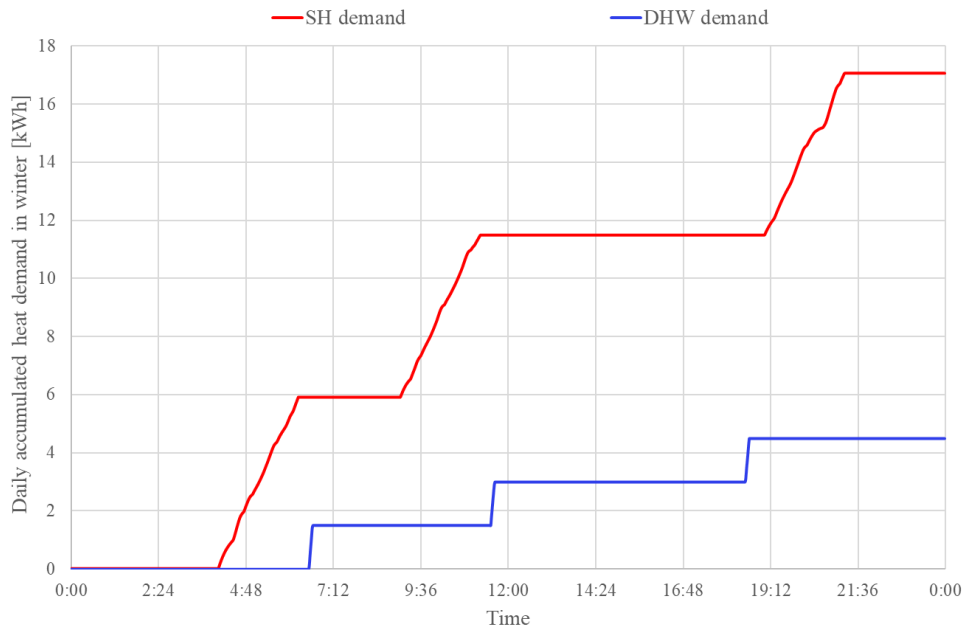20 dynamic thermal performance of the different loops.

A National Instrument cRIO with 9214 and 9403 cards was used for the data logging. The

measurement equipment and measurement accuracy in the presented experiment were described in

details in previous publication[49]. The SGHP system was tested under real weather conditions in

2019 except break of 5 days due to power failures caused by maintenances and renovations issues,

inclusive one day in March and 4 days in July. The thermal behavior of the combi-storage in

different operating conditions was analyzed based on the dynamic relation between the heat inputs

(solar energy/ground energy) and heating demands (DHW/SH) in the whole year.

2.2 The tank-in-tank combi-storage

2.2.1 The layout of the combi-storage and temperature sensors

The tank-in-tank combi-storage with five circuits is applied in the SGHP system, see Fig.4. The

combi-storage is divided into the inner tank for DHW and the outer tank for SH. To minimize heat

loss to indoor environment, the combi-storage was insulated with mineral wool with a thermal

conductivity of 0.45 W/(m·K). The entire insulated tank was covered by aluminum foil. The

insulation thickness on the top and the side of the tank is 200 mm and 50 mm respectively. The
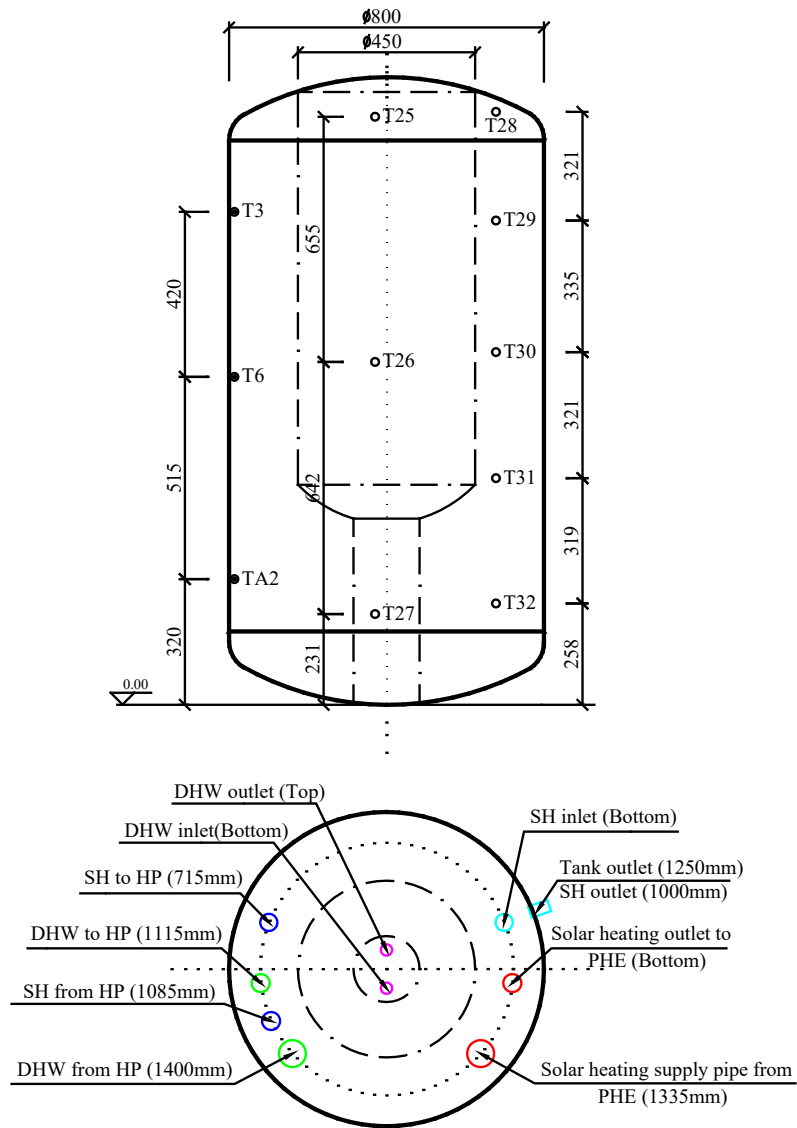
bottom of the tank is not insulated.

Fig.4 The tank-in-tank combi-storage with five circuits

The capability to achieve and maintain thermal stratification within the storage is particularly

crucial for combi-storages, and of utmost importance if a heat pump is used to charge this storage.

In order to secure a high degree of thermal stratification in the combi-storage during charge by solar

energy, an inlet stratifier is mounted at the bottom of the storage for the solar collector loop, see Fig.

2(a) and Fig. 4. The inlet stratifier is a polypropylene pipe with lockable openings acting as "non-

return" valves[32]. Four inlet/outlet pipes with variable heights are mounted at the bottom of the

storage and connected to the ground heat pump. The heights of the inlet/outlet pipes are especially

designed to maintain thermal stratification in the tank during charge by the ground source heat

pump. There are two inlet/outlet ports: one in the inner tank for DHW and one in the outer tank for

1 SH. With the arrangement of heights of the ports, water in the top of the inner tank usually has a

2 high temperature, therefore is used for DHW, while water in the middle of the outer tank has a

3 relatively lower temperature, therefore is used for SH. DHW production has a higher priority than

4 SH production in the load side of the heat pump. The return from the SH loop is led into the tank

5 via a direct inlet located under a half ball baffle plate in order to avoid mixing in the combi-storage.

6 Except the outlet to the SH loop, all inlet and outlet pipes go through the bottom of the combi-

7 storage.

8 *2.2.2 Operation and control*

9 Thermal conditions of the combi-storage are dynamically influenced by the interaction of solar

10 energy and ground energy, therefore optimized control of the system is necessary in order to utilize

11 energy in the best way. The temperature sensors TA2, T3 and T6 were used to control the responses

12 of the two heat sources to heat demands by comparing with the temperature sensor TA1 located at

13 the top of solar collector. A detailed description of the control strategies was presented in previous

14 publication[49], and Fig.5 illustrates the framework of controlling strategies.

15
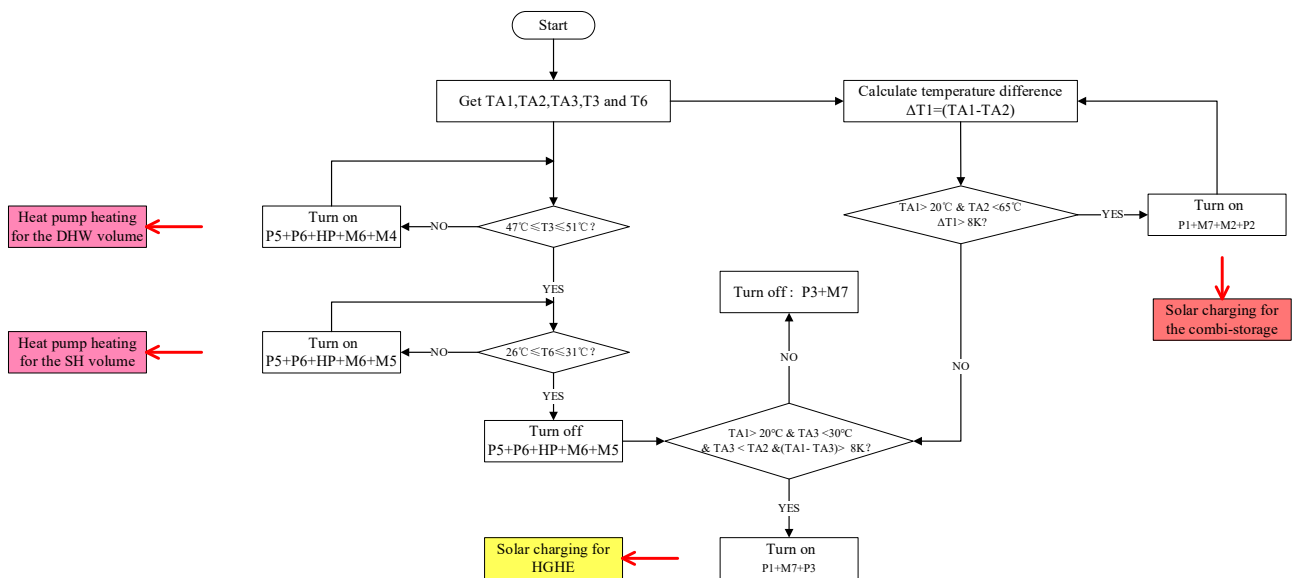
16 **Fig.5** The framework of controlling strategies of SGHP system

3. The analysis method

In order to analyze the thermal behavior of the combi-storage in the SGHP system, energy flow is essential for its performance assessment under the given operating conditions. The energy input and output in the different loops can be calculated as:

$$\dot{Q} = \rho V c_p (T_{in} - T_{out}) \tag{1}$$

Where hot water dynamic physical properties with transient temperature are described as [28]:

$$\rho(T) = 1000.6 - 0.0128 T^{1.76} \tag{2}$$

$$c_p(T) = 4209.1 - 1.328T + 0.01432T^2 \tag{3}$$

For the combi-stroage, the tank temperature T_{avg} is defined by mass weighted average temperature of the tank based on measurement of the temperature sensors T25~T32 shown in Fig.4.

4. Results and discussion

4.1 Daily operating modes of SGHP system based on the dynamic energy flows in the combi-storage

4.1.1 Operation modes

Based on the measured temperature differences and flow rates in the solar heating loop and the auxiliary loop, daily energy quantities charged to and discharged from the combi-storage were summarized. Based on the source of the heat, five types of typical days were identified:

- Single solar energy (SSE): Energy for heating the combi-storage is only from the solar heating loop.

- Single heat pump (SHP): Energy for heating the combi-storage is only from the auxiliary loop operated by the heat pump system.

- Single combi-storage (STA): No energy is used for heating the combi-storage in the whole day.

- The mixed mode: Both solar energy and ground heat are present in different parts of the

day. The days of mixed mode can be further divided into two typical days: The solar energy

dominant day (SSD) and the ground heat dominant day (SGD). SSD is defined for the day when the

solar energy is larger than the ground heat energy. Correspondingly, for the day when the ground

heat energy is higher than the solar energy, the operating mode is defined as the ground heat

dominant day (SGD).

4.1.2 Investigation on operation modes

The investigation on the two energy flows in the combi-storage was carried out for 2019, and the

monthly distribution of the operating modes is shown in Fig.6. January and December have only

two operation modes (SHP+ SGD) since the ground source heat pump was undoubtedly the

dominant heat source when there were a high heating demand and a low solar irradiation.

Three types of operation modes existed from February to April, and SSD occurred on the basis of

SHP and SGD as the heating demand decreased and solar irradiation increased in the first two

months. In April with the highest solar irradiation, the heating demand obviously decreased. Solar

energy became the dominant heat source and STA accounted for 23.3% of the days, which made the

monthly SPFs (5.7) the maximum in the whole year. In the three months (from May to July) with

almost the same heating demand, four types of operation modes occurred. SPFs in June was higher

because of the lower share of ground heat energy and the higher solar irradiation. In the other five

months with all the operation modes, the number of days with SHP increased with an increase of

heating demand and a decrease of solar irradiation, and more ground heat energy was used for

heating the combi-storage.

In the year 2019, 29.5% of the days can be categorized as SSE, which was mainly seen from

April to October with low heating load and high solar irradiation. On the contrary, 25.6% of the

days of SHP was concentrated in the period of high heating load and low solar irradiation. The

combining mode has the highest contribution (35.6% of the days), which was seen in every month,

of which, SSD existed in 10 months of the year with a contribution of 12.2%, SGD has a higher

contribution of 23.3%. Surprisingly, it was observed that the number of days on STA was up to

1   9.4%, which means the stored heat in the combi-storage can cover the heating demand in 34 days of

2   the year. In the presented valid experiment of 360 days, solar and ground energy alternated

3   dominance as the main energy source. The solar collector loop was active in 235 days, and the

4   number of days with active auxiliary loop for the ground source heat pump system was 220 days.
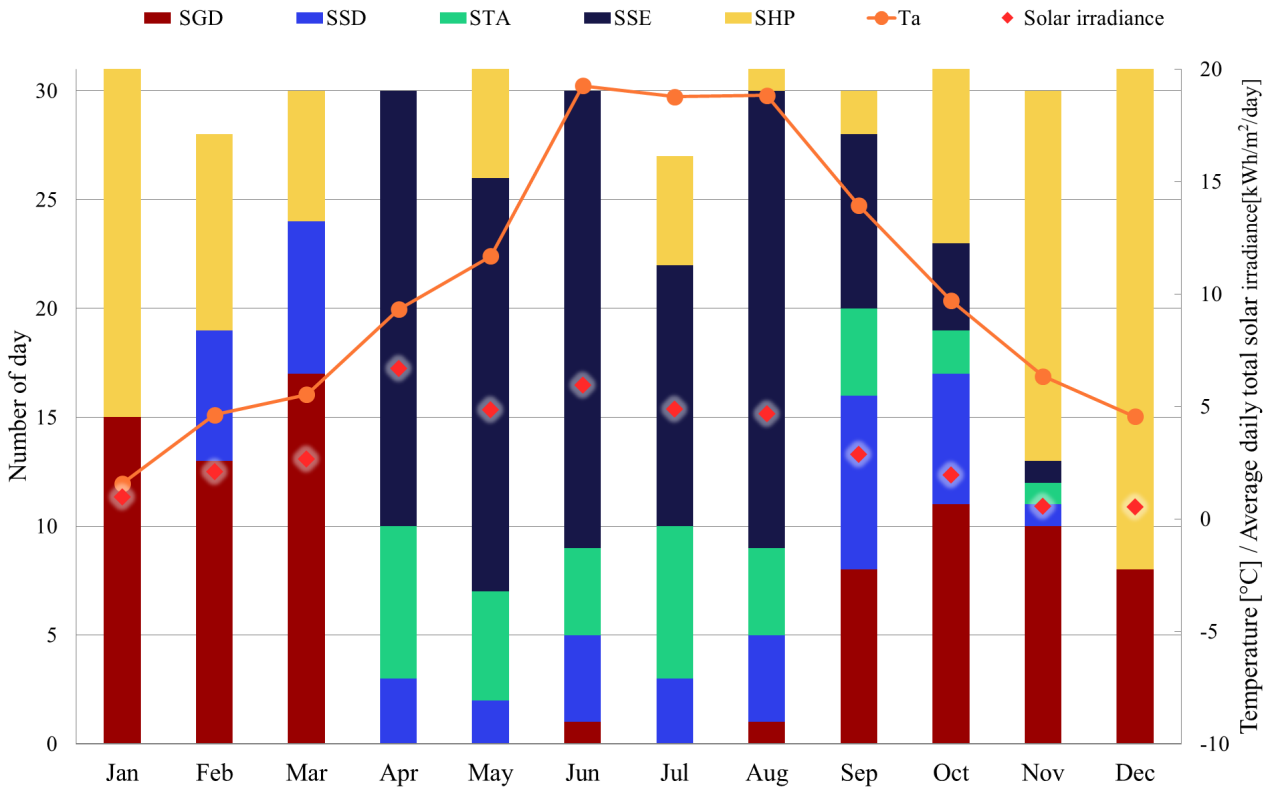
5

6   a) The distribution of monthly working modes and the corresponding solar irradiance
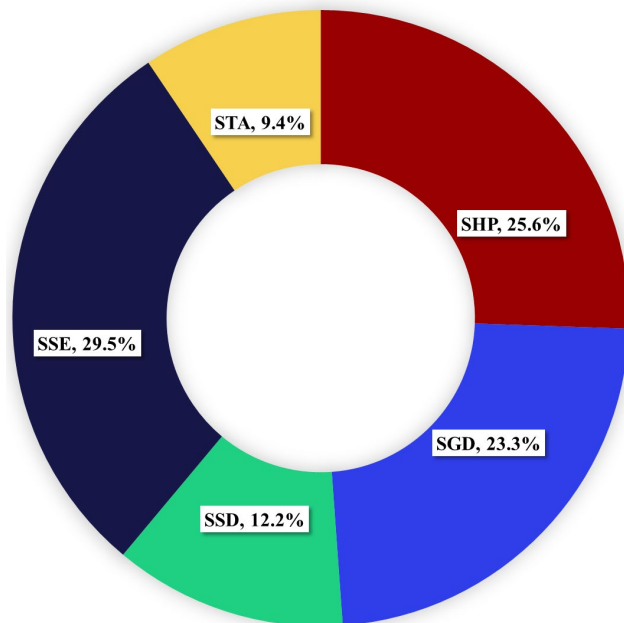
7

8   b) The yearly working modes distribution

4.2 Energy flow statuses on the five typical operation days

Based on the operation modes, the measured data were used to analyze the thermal behavior of

the combi-storage in the five typical days. The daily energy flows are illustrated in Table.2. As the

energy input of the combi-storage, solar energy and ground energy were compared. In the modes of

SSE, SSD and STA, high solar irradiance and low heating demand made the average water

temperatures higher than 50°C, and the surplus solar energy were used to charge the ground. For

the modes of SGD and SHP, due to operation of the heat pump, the combi-storage had relatively

lower average temperatures in the storage (31°C -32°C).

Table 2 The measured energy flows in the five typical operation days

Operation mode	$Q_{sol,tank}$	$Q_{HP,tank}$	Q_{SH}	Q_{DHW}	T_{avg}	$Q_{sol,ground}$	Date
	kWh	kWh	kWh	kWh	°C	kWh	
SSE	21.8	0	0	4.98	54.91	7.82	2019.4.4
SSD	23.3	2.51	0	5.21	53.1	3.51	2019.7.23
SGD	1.49	16.9	9.66	4.82	31.9	0.47	2019.11.29
SHP	0	27.65	17.87	4.8	31.02	0	2019.12.23
STA	0	0	0	5.12	54.94	37.2	2019.7.9

4.3 Thermal behavior on typical SSE/SSD days

In spring/summer of Denmark, high solar irradiance and long daylight hours make it possible for

solar energy to fully charge the combi-storage. Afterwards, the ground will be charged. The heat

pump operates only in individual cloudy and rainy days. Furthermore, more surplus solar energy is

used to charge the ground when SH load gradually decreases to zero. Solar energy is the dominant

heat source, consequently the average temperature of the combi-storage is kept at a higher level.

4.3.1 Dynamic responses of the tank for SSE

As a typical SSE day, the measured data on 4, April was used to analyze the thermal response of

the combi-storage. As shown in Tab.2, 74% (21.8kWh) of the produced solar energy was used to

charge the combi-storage, and the rest (only 7.82 kWh) was used to charge the ground. A daily

DHW consumption of 4.98 kWh was taken from the combi-storage. The DHW consumption was

equally distributed into three draw-offs: 6:13~6:19, 11:11~11:16 and 18:10~18:14.

According to the controlling strategy in Fig.5, both T3 and T6 were within the setting

temperature range, the HGHE and the combi-storage were charged in turn by solar energy based on

the relations between TA1, TA2 and TA3. Fig.7 shows the dynamic variations of water

temperatures and flow rates in a typical SEE day. With an increase of solar irradiance, solar energy

was firstly used to charge the ground from 7:07 to 9:36 by starting P3 and M7. The ground was also

charged again from 16:37 to 16:46. The maximum temperature difference between the outlet and

inlet of HGHE is up to 5.4 K at 9:36 before solar energy was used to charge to the tank.

For the SH volume in the combi-storage, the three temperatures (T30~T32) began to drop after

the first DHW draw-off at 6:13 until the solar circulating pump P2 was activated. During solar

charge of the SH volume from 9:37 to 16:36, water temperatures in the tank increased slowly until

the weighted average temperature reached 66.9 ℃ at 16:36. The impact of DHW draw-offs on

water temperatures of the SH volume can be seen in Fig.7. The effect of the first draw-off is much

larger than that of the third one due to the lower weighted average temperature in the morning.

Limited influence is observed in the second draw-off because the tank was charged by solar heat

simultaneously. After the third draw-off , the upper part of the tank had a temperature around 65℃.

Thermal stratification started to build up in the SH volume due to heat transfer from the SH volume

to the DHW volume of the tank. The temperature difference between T28 and T30 reached nearly 3

K at 24:00.

Water temperatures in the DHW volume of the combi-storage during a typical SSE day are

shown in Fig.7. There are three sudden drops of the water temperature at the bottom of the tank

(T27) corresponding to three DHW draw-offs. 21.8 kWh of solar energy was charged to the tank,

and it was higher than the daily DHW load. Consequently T25 increased from 49.6℃ to 65.2℃,

and T27 increased from 44.8℃ to 59.3℃. The difference between T25 and T27 is about 5.9 K at

24:00, and it is 1 K higher than at the start of the day.
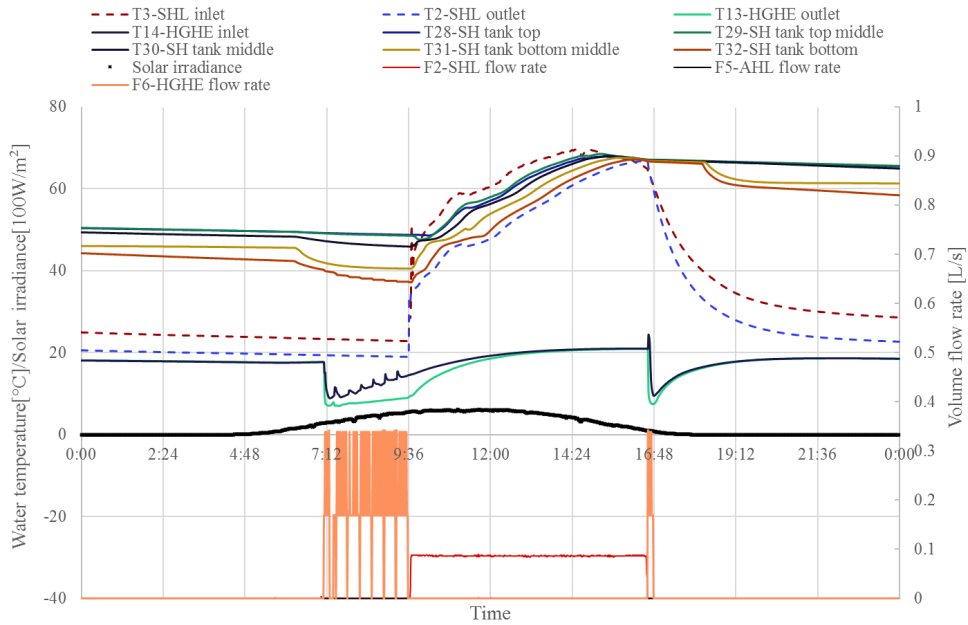
a) The thermal responses of the SH volume
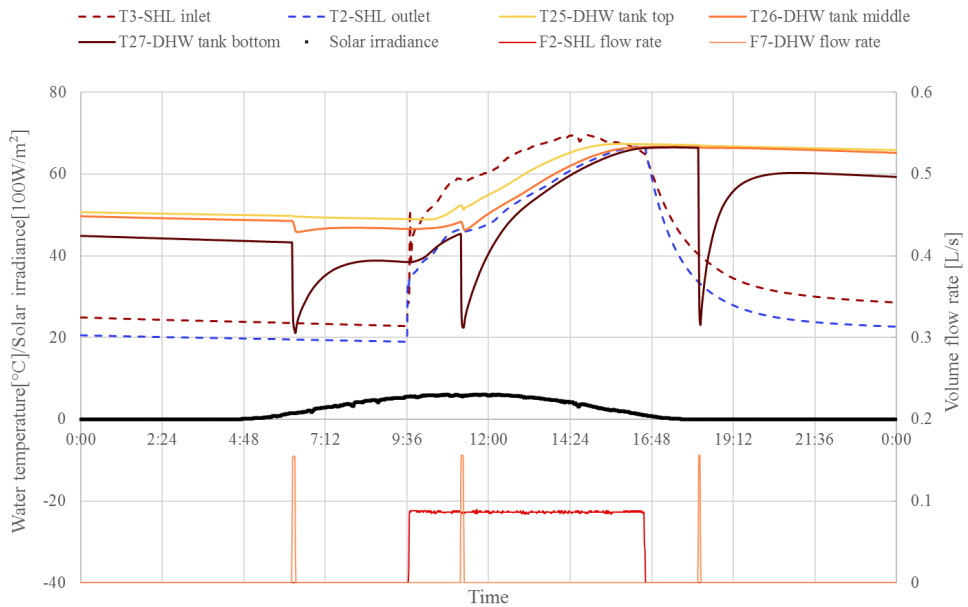
b) The thermal responses of the DHW volume

Fig.7 The thermal behavior of the combi-storage in a typical SSE day

1) Dimensionless temperature distribution

The dynamic vertical temperature distribution in the period of solar charge is used to analyze the thermal response of the combi-storage. The measurements are shown with dimensionless temperatures on the x-axis and the height of the tank on the y-axis. The dynamic vertical temperature distribution is shown in Fig.8. In order to eliminate the interference of the start temperatures ($T32_{start}$) and the inlet temperature (T3) in the analysis, the dimensionless temperature is used and defined as follows:
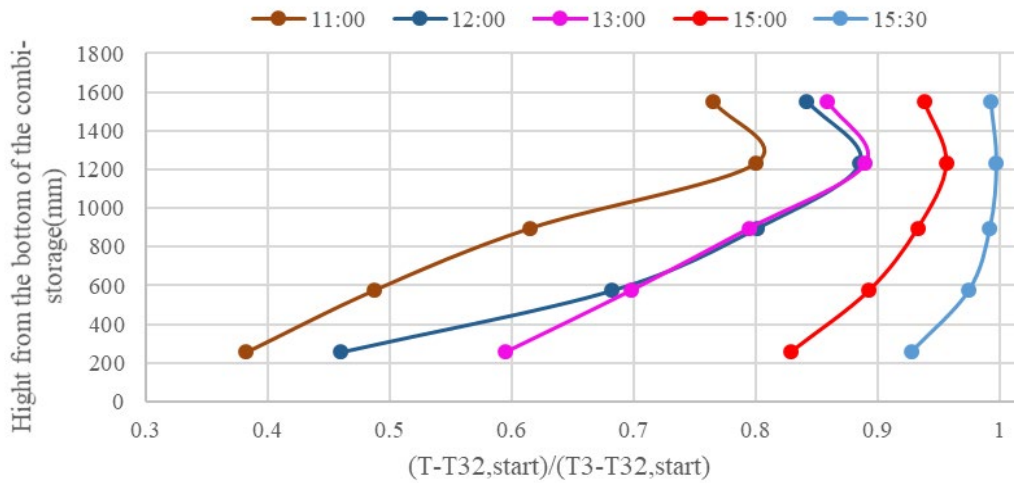
18

$$\Theta_{\text{SH}} = \frac{T - T32_{\text{start}}}{T3 - T32_{\text{start}}} \qquad (4)$$

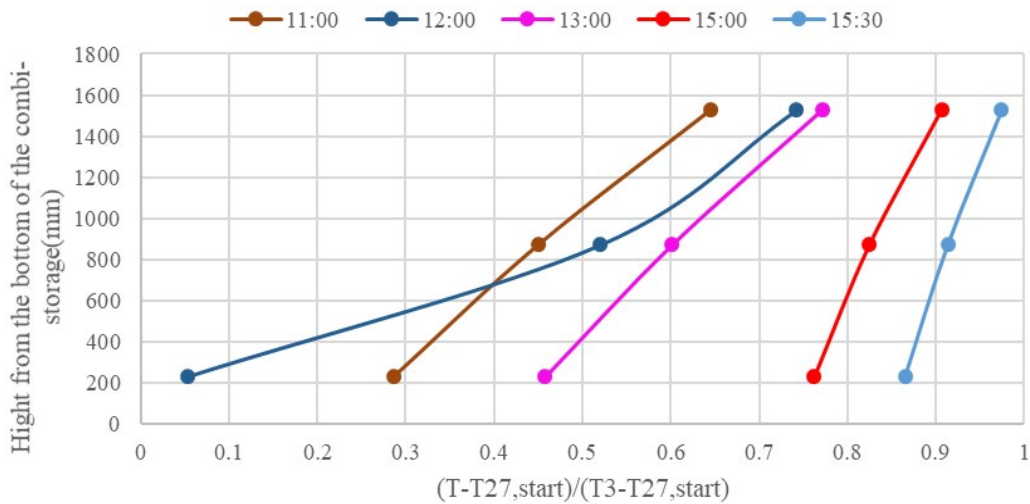$$\Theta_{\text{DHW}} = \frac{T - T27_{\text{start}}}{T3 - T27_{\text{start}}} \qquad (5)$$

Where T is water temperature at different heights of the tank, °C. T3 is the transient inlet

temperature of thermal stratifier, °C , and $T32_{\text{start}}$ and $T27_{\text{start}}$ is respectively the bottom temperature

of SH volume and DHW volume before the start of the charge by solar energy, °C.

a) Dimensionless temperature profiles of the SH volume

b) Dimensionless temperature profiles of the DHW volume

Fig.8 Dimensionless temperature profiles in the combi-storage in a typical SSE day

As shown in Fig.8, the highest temperature of the tank in SH volume was located near the top

of the stratifier (T29 shown in Fig.4). The vertical temperature gradient was effectively decreased

from 11:00 to 15:30 with continuous solar charge. T32 in the bottom of SH volume at 12:00 was still lower after 45-minute continuously solar charge due to the second DHW draw off. The slightly increased extents in the upper and middle temperatures (T28/T29/T30/T31) were observed from 12:00 to 13:00, and T32 increased because solar energy was effectively used to heat the bottom part. Due to maximum temperature deviation from T3 in the lower part, more charging effect was observed from 11:00 to 15:30, which made the vertical temperature gradient lower at 15:30.

Thermal stratification was orderly presented in the DHW volume in Fig.8. The vertical temperature gradient at 11:00 was same with that at 13:00, and large vertical temperature gradient was observed due to the second draw off at 11:11. 45-minute continuous solar charging caused the temperature gradient at 12:00 to resume the same level of 11:00. The continuously 2-hour heating process decreased the vertical temperature gradient at 15:00, and the temperature difference between T25 in the upper part and T27 in the bottom was further reduced.
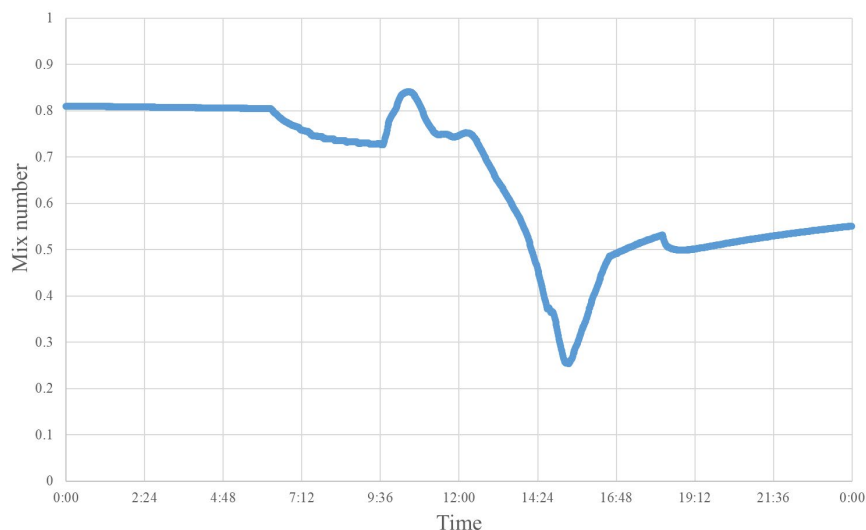
2) MIX number

The *MIX* number is useful for evaluating the thermal stratification in the combi-storage at a specific time and ranges from 0 to 1 which reflects the degree of stratification independent of the working conditions. The *MIX* number was defined as[50]:

$$MIX = \frac{M_{str} - M_{exp}}{M_{str} - M_{full\text{-}mixed}} \tag{6}$$

The energy-momentum content M_{exp} is related to the energy-momentum content of two theoretical cases, a perfectly stratified water tank (M_{str}) and a fully mixed water tank ($M_{full\text{-}mixed}$) with both storing the same amount of energy in the experimental tank. The *MIX* number varies from 0 to 1, where 0 represents a perfectly stratified tank and 1 represents a fully mixed tank. The three energy-momentum contents were described in details in Ref [51]. To calculate *MIX* numbers of different typical operation day, the temperatures of hot water and cold water were respectively set 70 °C and 20 °C to obtain their energy-momentum contents.
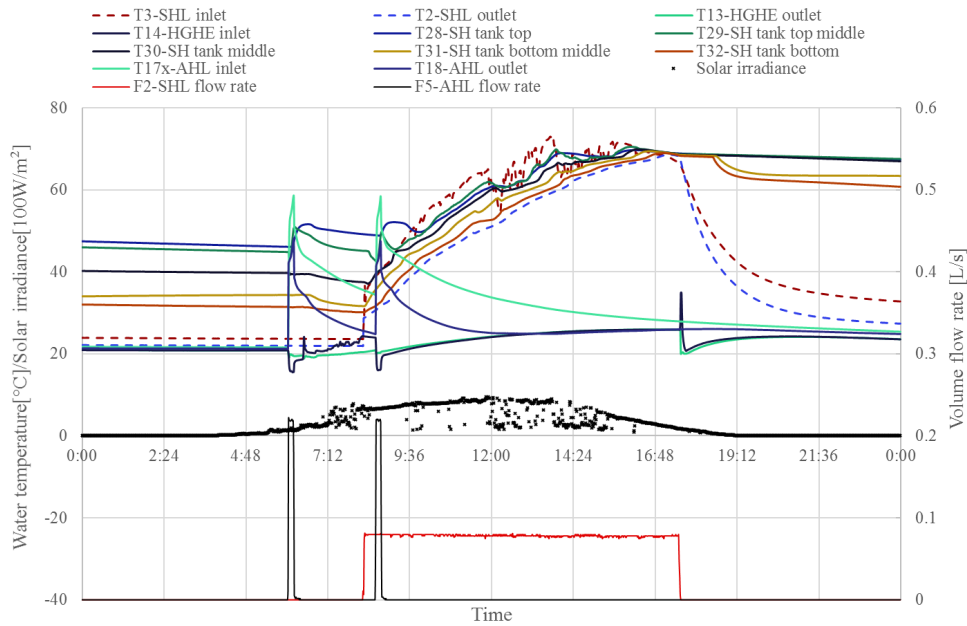
1 *MIX* numbers in the SH volume in the whole day are shown in Fig.9. The *MIX* number was

2 almost constant (0.8) when the first DHW draw-off finished at 6:19, and it decreased slowly to 0.73

3 until the solar charge was activated at 9:37. In the process of solar charge of the combi-storage from

4 9:37 to 16:36, the *MIX* number increased with the continuous charge from 9:37, and it was up to

5 0.84 of the maximum value at 10:31. The *MIX* number was kept higher than 0.8 from 10:02 to

6 10:52, and the energy discharge in the second DHW draw-off at 11:11 was much lower than the

7 solar charge in this period, thermal stratification is fully decided by the outlet water temperature of

8 solar heating supply pipe from PHE, and it is hardly influenced by the 6-minute DHW draw-off.

9 Since 12:19, the sharp decrease of *MIX* number was observed until *MIX* number decreased to the

10 lowest value of 0.25 at 15:21, which reflects thermal stratification established quickly with

11 continuous solar charge due to higher solar irradiance. As solar energy diffused in the combi-

12 storage and solar radiation decreased after 15:21, the five temperatures (T28~T32) shown in Fig.7(a)

13 were almost the same in SH volume until 18:14, the increase of *MIX* number reflects the thermal

14 stratification destroyed gradually and uniform vertical temperature distribution formed in the

15 storage. Though the third DHW draw-off finished at 18:14 caused *MIX* number decrease from 0.53

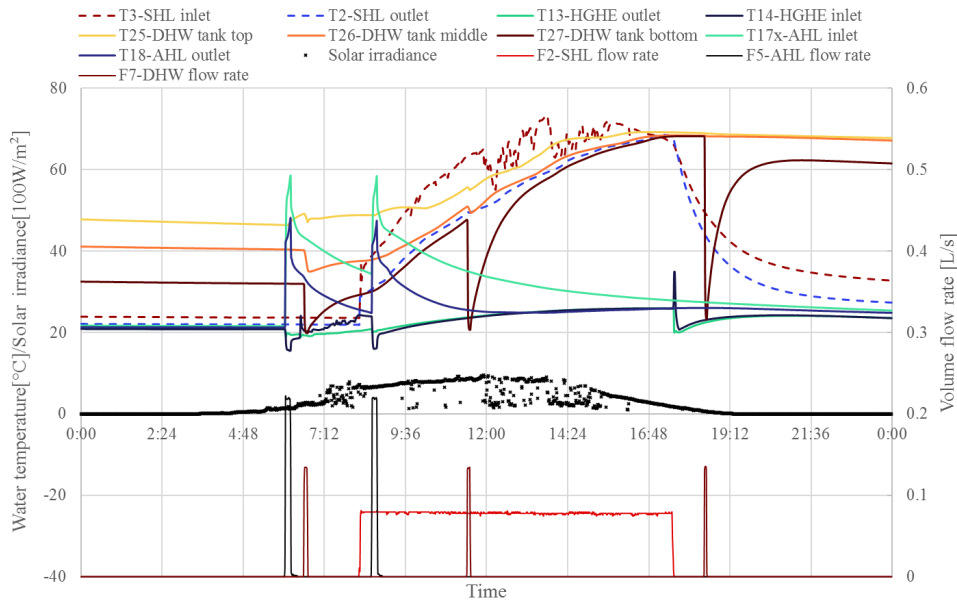16 to 0.5, the *MIX* number still increased to 0.55 at 24:00.

17

18 **Fig.9** *MIX* number variations in the SH volume in the typical SSE day

1   *4.3.2 Dynamic responses of the tank for SSD*

2   The measured data on July 23 was used to analyze thermal response of the combi-storage in a

3   typical SSD day. Fig.10 shows water temperatures and flow rates in a typical SSD day. Different

4   from SSE, heat pump was activated to charge for the DHW volume at 6:00 because the monitored

5   T3 was lower than 47℃ based on the controlling strategy shown in Fig.5. T25, T28 and T29 in the

6   upper part increased significantly in 20-minute operation, while T28 and T29 were hardly changed

7   after the first draw-off for DHW at 6:36. However, the available solar heat activated at 8:17 was not

8   high enough to maintain monitored T3 to reach 47℃ of the low temperature limit at 8:36, heat

9   pump was activated for the second time. In the DHW volume, the temperatures distribution was

10   hardly affected by the fluctuations of the inlet water temperature (T3) in the charging process by

11   heat pump, the three temperatures (T25~T27) were more sensitive to solar charge.

12
13   a) The thermal responses of the SH volume

Legend:
- - - T3-SHL inlet
- - - T2-SHL outlet
——— T13-HGHE outlet
——— T14-HGHE inlet
——— T25-DHW tank top
——— T26-DHW tank middle
——— T27-DHW tank bottom
——— T17x-AHL inlet
——— T18-AHL outlet
· Solar irradiance
——— F2-SHL flow rate
——— F5-AHL flow rate
——— F7-DHW flow rate

2 b) The thermal responses of the DHW volume
3 **Fig.10** The thermal behavior of the combi-storage in a typical SSD day
4 *4.4 Thermal behavior on typical SHP/SGD days*

5 In autumn/winter of Denmark with a lower solar irradiance and short daylight hours, the

6 available solar energy is limited. Undoubtedly, ground energy becomes the dominating heat source.

7 As shown in Fig.5, operation of the heat pump is controlled using water temperatures T3 and T6 in

8 the combi-storage.

9 *4.4.1 Dynamic responses of the tank for SHP*

10 As a typical day on SHP, the measured data on 13, December was used to analyze thermal

11 response of the combi-storage. The temperature difference $\Delta T1=(TA1-TA2)$ was lower than 8 °C

12 due to lower solar irradiance in the day (see Fig.5). Solar energy was not used to charge the tank,

13 and the heat supply was fully provided by the heat pump. As shown in Tab.2, the heat output of the

14 heat pump was 27.6 kWh, 22.7 kWh of which was used to cover SH and DHW demand, the rest

15 was lost by means of heat loss from the combi-storage and the connection pipes. Since SH was

16 provided mostly on demand, there was no need to charge the storage to higher temperatures. The

17 weighted average temperature of the storage was 31°C, which was much lower than the average

18 temperature in solar energy dominating days (SSE/SSD). The dynamic variations of water

19 temperatures and flow rates of the storage in a typical SHP day are illustrated in Fig.11.

The same as the control strategy for DHW, the circulation for SH was activated 3 times over the day, and each operation time was about 74 minutes with the starting time 4:02/9:02/19:02. Corresponding to the short-term daylight and lower irradiance, the heat pump was activated 18 times as can be seen by the flow meter (F5) to meet the heating demand, 8 of which was for charging the DHW volume, and 12 of which were charging for the SH volume. It should be noted that switches between the DHW charging and the SH charging was controlled by the valves (M6+M4/M5) in the periods of 6:44~7:13 and 20:21~20:55.

The sensor T28 and T29 show water temperatures in the upper part of the SH volume. T29 was more sensitive to the heating flow, and its fluctuation magnitude was much larger than that of T28 though they had the same tendency. T28 was kept in the range from 47℃ to 51℃ to ensure the outlet temperature level of DHW. It was observed that T25 gradually increased to nearly 50℃ by heat pump after every DHW draw-off even in the cold winter. T30 shows temperature variations of the middle of the SH volume during the day. Since the outlet to the SH loop was located below the sensor T29 and above the sensor T30, T30 is more sensitive to the SH load than T29. Most of the activated heating process occurred in the period of SH load, and heat was transfer rapidly to meet the SH demand, which made the T30 fluctuations narrower than that of T29. T30 was kept the range from 26 °C to 31 °C in the heating process to ensure the outlet temperature level of SH. Meanwhile, the intermittent heating process made T26 gradually resumed to about 30 °C after every DHW draw-off. For the bottom of the SH volume, the temperature variation of T31 was consistent with that of T32, and they were hardly influenced by the two ways of heating the combi-storage. T27 in the bottom DHW volume is almost equal to the tap water temperature, the impact of thermal diffusion of heating process on bottom volume was weak.

Due to the difference of heat sources, it is difficult for heat pump to supply hot water temperature as high as solar collectors. As shown in Fig.5, the monitored temperature T3 is used to control the temperature level of DHW, and T6 for the temperature level of SH. Based on the thermal responses of T28 and T30, the two monitored temperature sensors at setting positon are competent for

1   controlling heat pump to charge different parts in the tank. The heating flow is respectively directed

2   to the different demand for temperature level using the two heating loops in the combi-storage, and

3   the perfect implementation effect of the setting control strategy for heat pump system over the day

4   is validated. However, it is inevitable for heat pump system to increase extra electricity

5   consumption due to frequent startup shown in Fig.11. The control strategy could be refined to avoid

6   frequent on/off operations, however, further investigations are necessary to determine the optimized

7   control parameters.
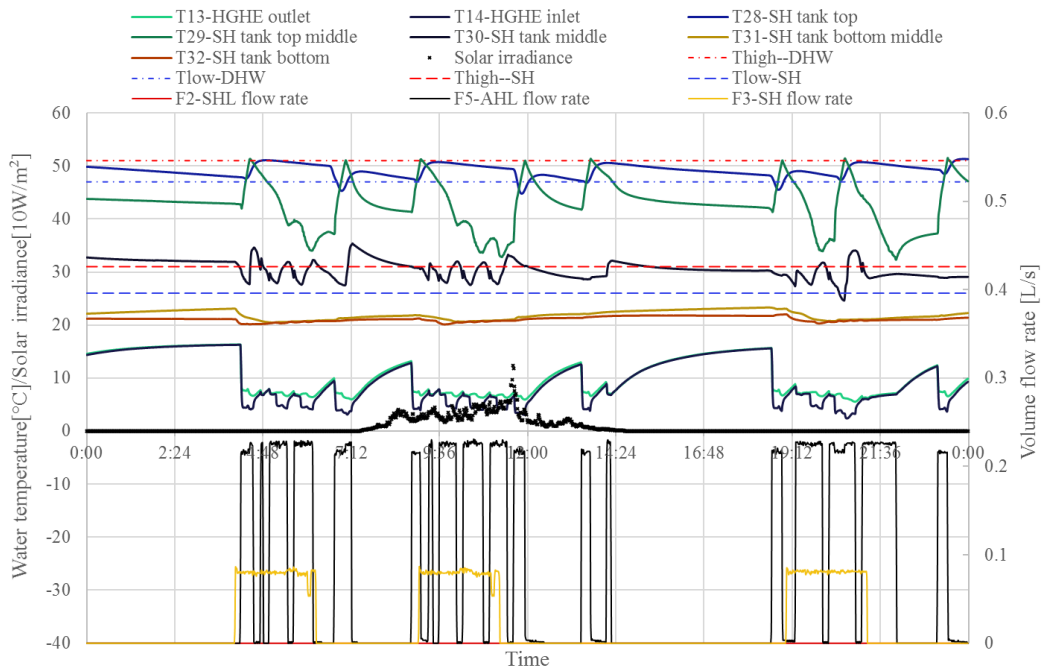
8
9   a) The thermal responses of the SH volume
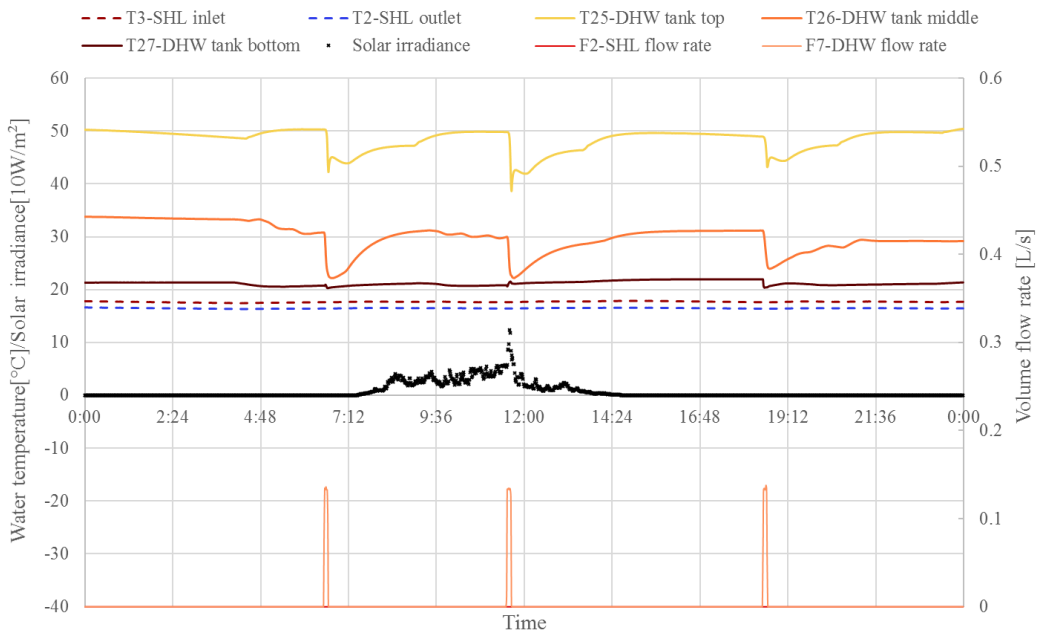
10
11   b) The thermal responses of the DHW volume
12   **Fig.11** The thermal behavior of the combi-storage in a typical SHP day

1

2   *MIX* numbers in the SH volume were calculated in the whole day, Fig.12 shows the dynamic

3   variations of *MIX* numbers. Thermal stratification was poor based on the oscillating *MIX* number in

4   the whole day though the upper and middle part were respectively charged by heat pump based on

5   the measured temperatures of T3 and T6. The *MIX* numbers were lower than 0.25, and it decreased

6   sharply corresponding to every intermittent charge, which indicates establishment of thermal

7   stratification in the storage. In the three periods of heating for SH, *MIX* number vibrated violently

8   with the frequent fluctuation of T30 due to the middle part of SH volume charged by heat pump.

9   The four increased tendencies of *MIX* numbers are observed during the standby periods: 0:00~4:04,

10   7:03~8:49, 11:56~13:30 and 13:51~18:40, and thermal stratification was better than the other

11   periods. In a word, the *MIX* numbers on SHP are much lower than that on SSE, thermal

12   stratification is fully applied in the charge for different volume by heat pump. Different from the

13   responses of water temperatures on SSE, water temperatures in the combi-storage were relatively

14   stable to meet for heating demand. As shown in Fig.11, the vertical temperature gradient in DHW

15   volume was almost constant over the day due to the two heating loops focusing on different place.

16   Therefore, heat pump system is indispensable to enhance the reliability of SGHP system.
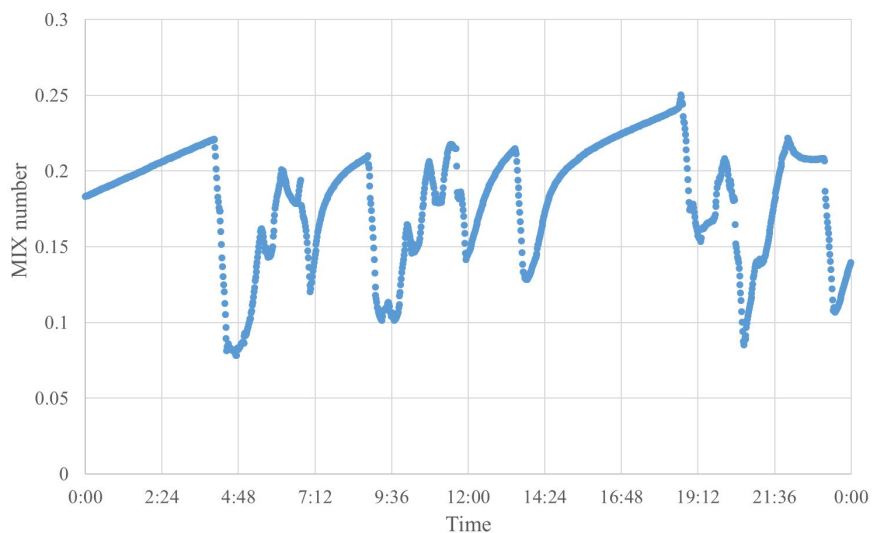

17
18   Fig.12 *MIX* number variations in the SH volume in a typical SHP day

19   *4.4.2 Dynamic responses of the tank for SGD*

20   The measured data on 29 November was used to analyze thermal response of the combi-storage

21   in a typical SGD day. The dynamic variations of water temperatures and flow rates on SGD are

1 illustrated in Fig.13. The heat pump was activated 11 times in order to meet the heating demand due

2 to the lower irradiance, which can be seen by the flow meter (F5). 7 of startups was for charging the

3 DHW volume, and 4 were for charging the SH volume. It should be noted that switches between the

4 DHW charging and the SH charging was controlled by the valves (M6+M4/M5) in the periods of

5 4:19~5:22 and 10:08~10:47. As for solar charging of the combi-storage, circulating pump P2 was

6 activated two times in the periods of 11:52~12:08 and 12:53~14:03 over the day. Due to the lower

7 solar irradiance, the increases of about 5℃ in T31 and T32 were observed at the end of the solar

8 charging, and the two temperatures decreased to about 21℃ after the 3rd 74-minute discharging for

9 SH demand. The supply water temperature for SH circulation was within 26℃~31℃, and it was

10 controlled in the range from 47℃ to 51℃ in the upper part of DHW volume. A relatively lower

11 temperature of the SH volume means a lower heat loss from the storage, which leads to a higher

12 efficiency of the system. The thermal behavior of the combi-storage proves that the control strategy

13 described in Fig.5 functions well. In DHW volume, T27 was increased by about 6.4℃ by solar

14 charging, and it fell to 21℃ until the 3rd draw-off for DHW. T25 and T26 were respectively

15 maintained at approx. 50 ℃ and 31 ℃, and they were hardly disturbed by solar charging.
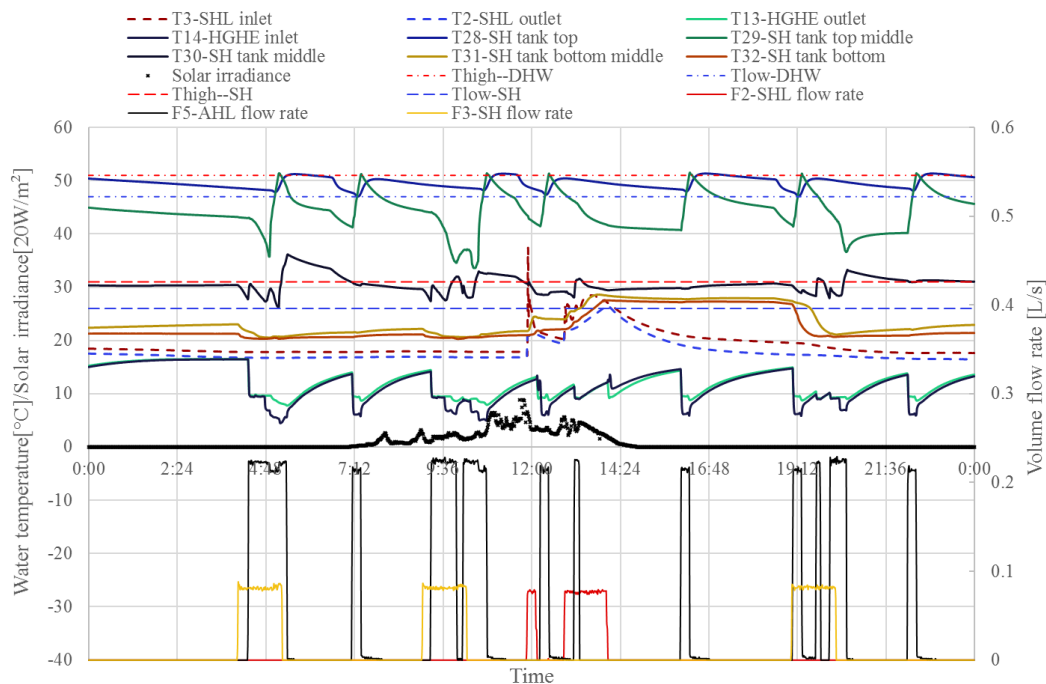
16
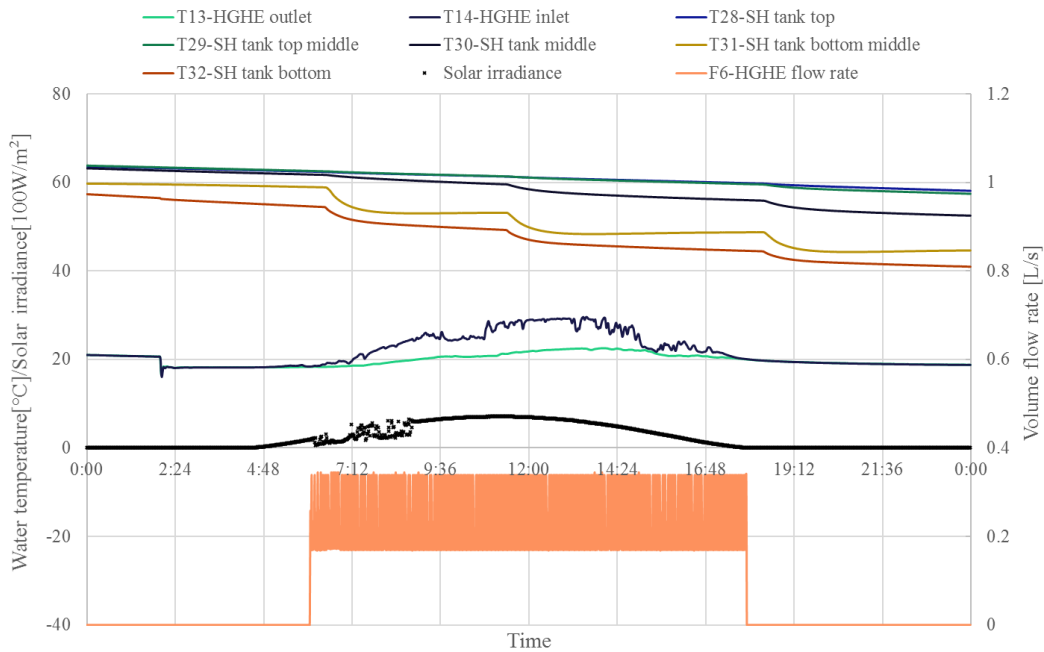17   a) The thermal responses of the SH volume
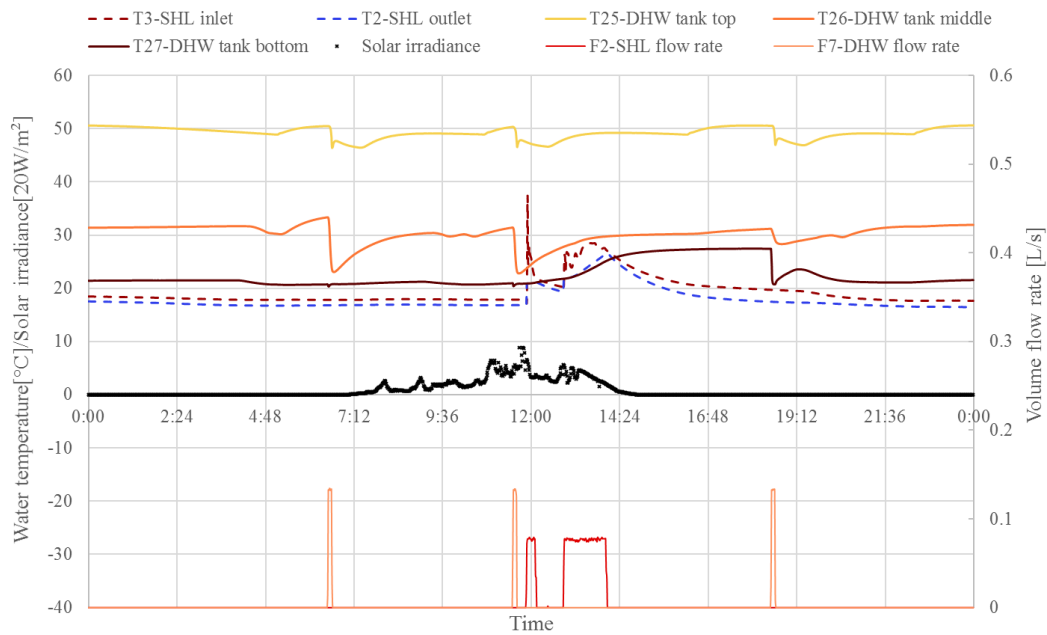
2
b) The thermal responses of the DHW volume
3
Fig.13 The thermal behavior of the combi-storage in a typical SGD day
4

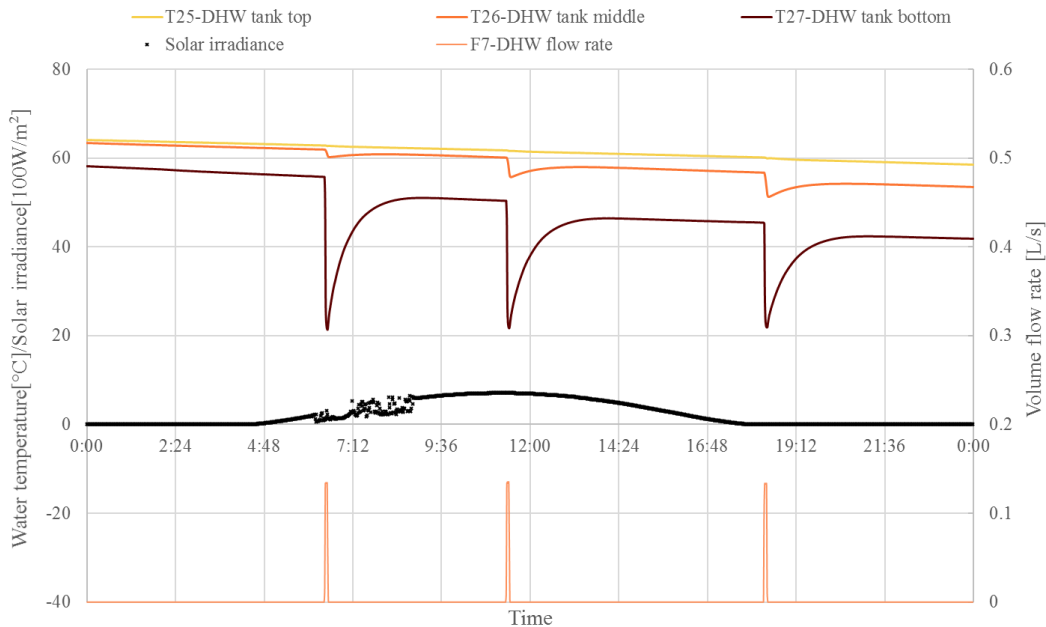5 *4.5 Thermal behavior on typical STA day*

6   Compared with the aforementioned four modes, STA is a coincidental state for the combi-storage

7 where no energy is used for heating the combi-storage in the whole day. The stored energy can meet

8 the daily heat demand. As shown in Fig.6, STA is widely located from April to November in 2019.

9 The measured data on 9, July was used to analyze the water temperatures responses to heat demand

10 on STA.

11   As described in Tab.2, the weighted average temperature was still up to 54.94℃ even though no

12 heating energy was charged to the combi-storage, only 5.12 kWh output was used for DHW. 37.2

13 kWh was fully charged to the ground by solar energy on the day due to higher solar irradiance. The

14 dynamic variations of water temperatures and flow rates in the day are illustrated in Fig.14.

15   The three draw-offs for DHW caused disturbances of the vertical temperature distribution. The

16 vertical temperature gradients in the two volumes increased due to cold inlet at the bottom of the

17 tank. Solar energy was used to charge the ground from 6:04 to 17:54 by use of HGHE because the

18 condition of activating pump P3 (TA1> 20°C & TA3 <30°C& TA3 < TA2 & (TA1- TA3)>8 K)

19 was met. The inlet water temperature of HGHE fluctuated with the variation of solar irradiance, and

20 the maximum inlet water temperature was 29.4 °C at 13:32

28

a) The thermal responses of the SH volume

b) The thermal responses of the DHW volume

Fig.14 The thermal behavior of the combi-storage in a typical STA day

The dynamic variations of *MIX* numbers in a typical STA day are illustrated in Fig.15. Three cliff

descents of *MIX* numbers were observed with the three DHW draw-offs. The *MIX* numbers

increased slowly after every draw-off, which showed that good thermal stratifications were

reconstructed in the standby periods due to no energy charge or discharge. In the whole day, the

MIX number decreased from 0.64 to 0.6, and the decreased ratios of *MIX* number were reduced with

the corresponding DHW draw-off, thermal stratification was getting clearer with energy discharge.
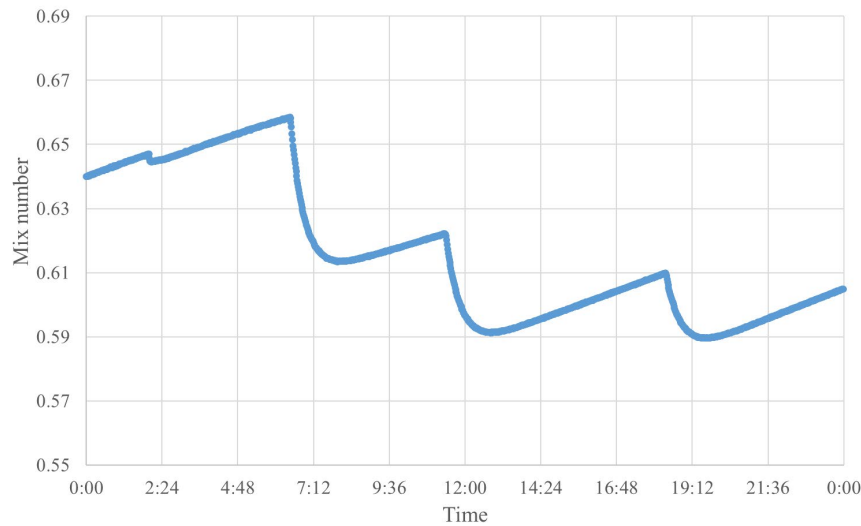
Fig.15 *MIX* number variations in the SH volume in a typical STA day

4.6 Final discussion

Based on the analysis on the *MIX* numbers in the three typical days (SSE/SHP/STA), the *MIX*

numbers in the typical SHP day were lower than that of the two typical days. The four variable-

height inlet/outlet pipes connected to the ground heat pump ensured good thermal stratification in

the combi-storage under the maximum energy discharge. The *MIX* numbers before 12:00 were

higher than 0.7 in the typical SSE day, which proved that solar heat diffused rapidly to ensure the

fully mixed tank. The stored heat can make thermal stratification better after every DHW draw-off

in the typical STA day, which was validated by the variations of *MIX* numbers within 0.66~0.59.

Installed with temperature sensors, the combi-storage was designed to control how to activate

solar energy or ground heat energy based on the measured water temperature responses at the

different positions. For the combi-storage, the three heating loops and temperature sensors'

positions were not optimal for thermal stratification, the insulation status also reduced the

effectiveness of the control strategy of SGHP system. More experimental and simulation

investigations should be made to improve the system performance, for example, by optimizing the

design of the three heating loops and temperature sensors' positions corresponding to the control

strategies in Fig.5.

5. Conclusions

The combi-storage played an important role in the SGHP system for a single-family house in the whole year. Based on the operation modes classified by the contribution of energy input in 2019, this paper presented experimental investigation on thermal behavior of the combi-storage and the influence of the control strategy. The following conclusions are drawn:

1) Five operation modes were identified for the combi-storage based on the contribution of the different heating source in 2019. Based on the analysis on the distribution of the working mode over the year, it is proven that the functions of the combi-storage were fully realized, inclusive peak shaving, storage of surplus solar heat and operational reliability of the SGHP system.

2) For the daily operation mode in 2019, 29.5% of the days on SSE was higher than that on SHP, and the mixed mode (SGD/SSD) accounted for 35.5% of the total experimental days. The number of days on STA was up to 9.4%, it means the combi-storage can meet the heating demand using accumulated heat in 34 days of the whole year.

3) On SSE/SSD, the solar energy was firstly used to charge the combi-storage, and secondly charged the ground as the heat source of the heat pump system. Solar energy provided fully heating flows for the whole tank on SSE/SSD mode. On SSE operation mode, the maximum *MIX* number was 0.66 at 10:38, and thermal stratifier made the vertical temperature distribution uniform and the temperatures were all up to about 68 ℃ at the end of the solar heating process.

4) On SHP/SGD, the two heating loops at different position provided effective heating flows for the DHW volume and the SH volume with the ground heat pump system. The vertical temperature gradient in the combi-storage is larger than that on SSE/SSD. On SHP operation mode, all *MIX* numbers are lower than 0.25. The middle of the combi-storage (T30) was kept in the temperature range from 26 ℃ to 31 ℃ in the heating process to ensure the outlet temperature level of SH, and the temperature of the top of the DHW volume (T25) was within 47 ℃~51 ℃. The different temperature levels for DHW and SH are obtained using the intermittent operation of heat pump system under the setting control strategy.

5) On STA, neither solar energy nor ground heat energy was used to charge the combi-storage. The three draw-offs for DHW caused the top temperature (T25) linearly declined from 64.04 ℃ to 58.5 ℃, the stepped drops of the middle temperature (T26) from 63.4 ℃ to 53.5 ℃ and the bottom temperature (T27) from 58.1 ℃ to 41.8 ℃. The *MIX* number in SH volume decreased from 0.58 to 0.285 after three cliff descents made by the corresponding DHW draw-offs. The accumulated thermal energy in the combi-storage can meet for the daily heating demand on STA operation mode.

For future work, the experimental results will be further compared to the relative studies on the SGHP system. A simulation model of the SGHP system inclusive the tank-in-tank combi-storage will be developed. Thermal behavior of the combi-storage will be used to validate the model. Furthermore, the validated model will be used for design optimization and dimensioning of the combi-storage in other solar heating systems.

Acknowledgements

References

[1]   C. Zhang, S. Hu, Y. Liu, Q. Wang, Optimal design of borehole heat exchangers based on hourly load simulation, Energy. 116 (2016) 1180–1190. https://doi.org/10.1016/j.energy.2016.10.045.

[2]   A. Balbay, M. Esen, Experimental investigation of using ground source heat pump system for snow melting on pavements and bridge decks, Scientific Research and Essays. 5 (2010) 3955–3966.

1   [3]   A. Balbay, M. Esen, Temperature distributions in pavement and bridge slabs heated by using

2   vertical ground-source heat pump systems, Acta Scientiarum. Technology. 35 (2013) 677–

3   685.

4   [4]   G. Liu, C. Li, S. Hu, Y. Ji, Z. Tong, Y. Wang, L. Tong, Z. Mao, S. Lu, Study on heat transfer

5   model of capillary exchanger in subway source heat pump system, Renewable Energy. 150

6   (2020) 1074–1088. https://doi.org/10.1016/j.renene.2019.10.112.

7   [5]   H. Esen, M. Inalli, M. Esen, Technoeconomic appraisal of a ground source heat pump system

8   for a heating season in eastern Turkey, Energy Conversion and Management. 47 (2006)

9   1281–1297. https://doi.org/10.1016/j.enconman.2005.06.024.

10   [6]   H. Esen, M. Inalli, M. Esen, A techno-economic comparison of ground-coupled and air-

11   coupled heat pump system for space cooling, Building and Environment. 42 (2007) 1955–

12   1965. https://doi.org/10.1016/j.buildenv.2006.04.007.

13   [7]   H. Esen, M. Inalli, M. Esen, Numerical and experimental analysis of a horizontal ground-

14   coupled heat pump system, Building and Environment. 42 (2007) 1126–1134.

15   https://doi.org/10.1016/j.buildenv.2005.11.027.

16   [8]   H. Esen, M. Inalli, M. Esen, K. Pihtili, Energy and exergy analysis of a ground-coupled heat

17   pump system with two horizontal ground heat exchangers, Building and Environment. 42

18   (2007) 3606–3615. https://doi.org/10.1016/j.buildenv.2006.10.014.

19   [9]   G. Hou, H. Taherian, L. Li, A predictive TRNSYS model for long-term operation of a hybrid

20   ground source heat pump system with innovative horizontal buried pipe type, Renewable

21   Energy. 151 (2020) 1046–1054. https://doi.org/10.1016/j.renene.2019.11.113.

22   [10] H. Esen, M. Inalli, A. Sengur, M. Esen, Modelling a ground-coupled heat pump system using

23   adaptive neuro-fuzzy inference systems, International Journal of Refrigeration. 31 (2008) 65–

24   74. https://doi.org/10.1016/j.ijrefrig.2007.06.007.

[11] H. Esen, M. Inalli, A. Sengur, M. Esen, Performance prediction of a ground-coupled heat pump system using artificial neural networks, Expert Systems with Applications. 35 (2008) 1940–1948. https://doi.org/10.1016/j.eswa.2007.08.081.

[12] H. Esen, M. Inalli, A. Sengur, M. Esen, Artificial neural networks and adaptive neuro-fuzzy assessments for ground-coupled heat pump system, Energy and Buildings. 40 (2008) 1074–1083. https://doi.org/10.1016/j.enbuild.2007.10.002.

[13] H. Esen, M. Inalli, A. Sengur, M. Esen, Predicting performance of a ground-source heat pump system using fuzzy weighted pre-processing-based ANFIS, Building and Environment. 43 (2008) 2178–2187. https://doi.org/10.1016/j.buildenv.2008.01.002.

[14] H. Esen, M. Inalli, A. Sengur, M. Esen, Forecasting of a ground-coupled heat pump performance using neural networks with statistical data weighting pre-processing, International Journal of Thermal Sciences. 47 (2008) 431–441. https://doi.org/10.1016/j.ijthermalsci.2007.03.004.

[15] H. Esen, M. Inalli, A. Sengur, M. Esen, Modeling a ground-coupled heat pump system by a support vector machine, Renewable Energy. 33 (2008) 1814–1823. https://doi.org/10.1016/j.renene.2007.09.025.

[16] M. Esen, H. Esen, Experimental investigation of a two-phase closed thermosyphon solar water heater, Solar Energy. 79 (2005) 459–468. https://doi.org/10.1016/j.solener.2005.01.001.

[17] M. Esen, Thermal performance of a solar cooker integrated vacuum-tube collector with heat pipes containing different refrigerants, Solar Energy. 76 (2004) 751–757. https://doi.org/10.1016/j.solener.2003.12.009.

[18] M. Esen, Thermal performance of a solar-aided latent heat store used for space heating by heat pump, Solar Energy. 69 (2000) 15–25. https://doi.org/10.1016/s0140-6701(01)80659-7.

[19] M.Y. Haller, D. Carbonell, I. Mojic, C. Winteler, E. Bertram, M. Bunea, W. Lerch, F. Ochs, Solar and heat pump systems - summary of simulation results of the IEA SHC task 44/HPP annex 38, 11th IEA Heat Pump Conference. (2014) 1–12.

[20] J.-C. Hadorn, Solar and heat pump systems for residential buildings, John Wiley & Sons, 2015.

[21] M. Esen, T. Yuksel, Experimental evaluation of using various renewable energy sources for heating a greenhouse, Energy and Buildings. 65 (2013) 340–351. https://doi.org/10.1016/j.enbuild.2013.06.018.

[22] C. Fraga, F. Mermoud, P. Hollmuller, E. Pampaloni, B. Lachal, Large solar driven heat pump system for a multifamily building: Long term in-situ monitoring, Solar Energy. 114 (2015) 427–439. https://doi.org/10.1016/j.solener.2015.01.039.

[23] M. Esen, T. Ayhan, Development of a model compatible with solar assisted cylindrical energy storage tank and variation of stored energy with time for different phase change materials, Energy Conversion and Management. 37 (1996) 1775–1785. https://doi.org/10.1016/0196-8904(96)00035-0.

[24] M. Esen, A. Durmuş, A. Durmuş, Geometric design of solar-aided latent heat store depending on various parameters and phase change materials, Solar Energy. 62 (1998) 19–28. https://doi.org/10.1016/S0038-092X(97)00104-7.

[25] J. Nicolas, J.P. Poncelet, Solar-assisted heat pump system and in-ground energy storage in a school building, Solar Energy. 40 (1988) 117–125. https://doi.org/10.1016/0038-092X(88)90079-5.

[26] L. Dai, S. Li, L. DuanMu, X. Li, Y. Shang, M. Dong, Experimental performance analysis of a solar assisted ground source heat pump system under different heating operation modes, Applied Thermal Engineering. 75 (2015) 325–333. https://doi.org/10.1016/j.applthermaleng.2014.09.061.

1 [27] S. Alizadeh, An experimental and numerical study of thermal stratification in a horizontal

2 cylindrical solar storage tank, Solar Energy. 66 (1999) 409–421.

3 [28] S. Furbo, Hot water tanks for solar heating systems, 2004. DTU Byg, Danmarks Tekniske

4 Universitet. Byg Rapport No. R-100 http://www.byg.dtu.dk/publications/rapporter/byg-

5 r100.pdf.

6 [29] S. Knudsen, Consumers' influence on the thermal performance of small SDHW systems -

7 Theoretical investigations, Solar Energy. 73 (2002) 33–42. https://doi.org/10.1016/S0038-

8 092X(02)00018-X.

9 [30] L.J. Shah, E. Andersen, S. Furbo, Theoretical and experimental investigations of inlet

10 stratifiers for solar storage tanks, Applied Thermal Engineering. 25 (2005) 2086–2099.

11 https://doi.org/10.1016/j.applthermaleng.2005.01.011.

12 [31] D. Erdemir, N. Altuntop, Improved thermal stratification with obstacles placed inside the

13 vertical mantled hot water tanks, Applied Thermal Engineering. 100 (2016) 20–29.

14 https://doi.org/10.1016/j.applthermaleng.2016.01.069.

15 [32] J. Dragsted, S. Furbo, M. Dannemand, F. Bava, Thermal stratification built up in hot water

16 tank with different inlet stratifiers, Solar Energy. 147 (2017) 414–425.

17 https://doi.org/10.1016/j.solener.2017.03.008.

18 [33] R. Padovan, M. Manzan, E.Z. De Zorzi, G. Gullì, A. Frazzica, Model development and

19 validation for a tank in tank water thermal storage for domestic application, Energy Procedia.

20 81 (2015) 74–81. https://doi.org/10.1016/j.egypro.2015.12.061.

21 [34] I.J. Moncho-esteve, M. Gasque, P. González-altozano, G. Palau-salvador, Simple inlet

22 devices and their influence on thermal stratification in a hot water storage tank, Energy &

23 Buildings. 150 (2017) 625–638. https://doi.org/10.1016/j.enbuild.2017.06.012.

24 [35] H. Drück, E. Hahne, Test and Comparison of Hot Water Stores for Solar Combisystems,

25 Eurosun '98. (1998).

1   [36]   T. Pauschinger, H. Drück, E. Hahne, Comparison Test of Solar Heating Systems for

2   Domestic, Hot Water Preparation and Space Heating, in: Proceeding of EuroSun, 1998.

3   [37]   U. Jordan, Untersuchung eines Solarspeichers zur kombinierten Trinkwassererwärmung und

4   Heizungsunterstützung, VDI-Verlag, 2002.

5   [38]   K. Lorenz, Kombisolvärmesystem, Utvärdering av möjliga systemförbättringar (Solar

6   combisystems, Evaluation of possible system improvements). Licentiate thesis. Institutionen

7   för installationsteknik, Chalmers University of Technology, Göteborg, Sweden, 2001,

8   (2001).

9   [39]   E. Andersen, L.J. Shah, S. Furbo, Thermal performance of danish solar combi systems in

10   practice and in theory, Journal of Solar Energy Engineering, Transactions of the ASME. 126

11   (2004) 744–749. https://doi.org/10.1115/1.1688381.

12   [40]   W. Durisch, F. Von Roth, W.J. Tobler, Advances in gas-fired thermophotovoltaic systems,

13   Journal of Solar Energy Engineering, Transactions of the ASME. 129 (2007) 416–422.

14   https://doi.org/10.1115/1.2770749.

15   [41]   E. Andersen, S. Furbo, Theoretical comparison of solar water/space-heating combi systems

16   and stratification design options, Journal of Solar Energy Engineering, Transactions of the

17   ASME. (2007). https://doi.org/10.1115/1.2770752.

18   [42]   H. Esen, M. Esen, O. Ozsolak, Modelling and experimental performance analysis of solar-

19   assisted ground source heat pump system, Journal of Experimental & Theoretical Artificial

20   Intelligence. 29 (2017) 1–17.

21   [43]   J. Bois, L. Mora, E. Wurtz, Energy saving analysis of a solar combi-system using detailed

22   control algorithm modeled with Modelica, Energy Procedia. 78 (2015) 1985–1990.

23   https://doi.org/10.1016/j.egypro.2015.11.389.

24   [44]   W. El-baz, P. Tzscheutschler, Experimental Study and Modeling of Ground-Source Heat

25   Pumps with Combi-Storage in Buildings, (2018). https://doi.org/10.3390/en11051174.

[45] M.Y. Haller, R. Haberl, I. Mojic, E. Frank, Hydraulic integration and control of heat pump and combi-storage : Same components , big differences, Energy Procedia. 48 (2014) 571–580. https://doi.org/10.1016/j.egypro.2014.02.067.

[46] E. Andersen, Z. Chen, J. Fan, S. Furbo, B. Perers, Investigations of intelligent solar heating systems for single family house, Energy Procedia. 48 (2014) 1–8. https://doi.org/10.1016/j.egypro.2014.02.002.

[47] TUV Rheinland/DIN CERTCO, Summary of EN 12975 Test Results , annex to Solar KEYMARK Certificate of Kingspan Thermomax solar collectors, (2011) 9–10.

[48] M. Dannemand, B. Perers, S. Furbo, Performance of a demonstration solar PVT assisted heat pump system with cold buffer storage and domestic hot water storage tanks, 189 (2019) 46–57.

[49] C. Zhang, E. Nielsen, J. Fan, S. Furbo, Q. Li, Experimental investigation on a combined solar and ground source heat pump system for a single-family house: Energy flow analysis and performance assessment, Energy and Buildings. (2021) 110958. https://doi.org/https://doi.org/10.1016/j.enbuild.2021.110958.

[50] A. Castell, M. Medrano, C. Solé, L.F. Cabeza, Dimensionless numbers used to characterize stratification in water tanks for discharging at low flow rates, Renewable Energy. 35 (2010) 2192–2199. https://doi.org/10.1016/j.renene.2010.03.020.

[51] Y. Bai, Z. Wang, J. Fan, M. Yang, Numerical and experimental study of an underground water pit for seasonal heat storage, Renewable Energy. 150 (2020) 487–508. https://doi.org/10.1016/j.renene.2019.12.080.

Nomenclature

c fluid specific heat (J/(kg °C))

Q energy input/output (kWh)

$\dot{Q}$ heat flow rate (kW)

M energy-momentum(J m)

MIX MIX number (--)

T temperature (°C)

t operating time (min)

V volumetric flow rate (m^3/s)

Greek symbols

ρ fluid density (kg/m^3)

Θ dimensionless temperature (--)

Subscripts

avg   average

exp   experiment

HP   heat pump

in   inlet fluid

mix   mixture

out   outlet fluid

p   pressure

s   system

str   stratification

sol   solar

Abbreviations

COP   coefficient of performance

CFD   Computational Fluid Dynamics

DHW   domestic hot water

GSHP   ground source heat pump

HGHE   horizontal ground heat exchanger

PIV   Particle Image Velocimetry

SDHW   solar domestic hot water

SSD   solar energy dominant

SGD   ground heat energy dominant

SGHP   solar and ground source heat pump

SH   space heating

SHP   single heat pump

SPF	season performance factor
SSE	single solar energy
STA	single combi-storage